2020 IEEE/RSJ International Conference on Intelligent Robots and Systems (IROS)
October 25-29, 2020, Las Vegas, NV, USA (Virtual)

OceanVoy: A Hybrid Energy Planning System for Autonomous Sailboat*

Qinbo Sun[2], Weimin Qi[2], Hengli Liu[1,3], Zhenglong Sun[1,2], Tin Lun Lam[1,2] and Huihuan Qian[1,2,†]

***Abstract*— Towards long range and high endurance sailing, energy is of utmost importance. Moreover, benefiting from the dominance of the sailboat itself, it is energy-saving and environment-friendly. Thus, the sailboat with energy planning problem is meaningful. However, until now, the sailboat energy optimization problem has rarely been considered. In this paper, we focus on the energy consumption optimization of an autonomous sailboat. It has been formulated as a Nonlinear Programming problem (NLP). We deal with it with a hybrid control scheme, in which pseudo-spectral (PS) optimal control method is used in heading control, and a model-free framework guided by Extreme Seeking Control (ESC) is used in sail control. The optimal path is generated with the optimal input motor torques in time series. As a result, both simulation and experiments have validated motion planning and energy planning performance. Notably, about 7% of energy is saved on average. Our proposed method can make sailboats sailing longer and sustainable.**

Fig. 1. OceanVoy is sailing in Shenxian Lake, the Chinese University of Hong Kong, Shenzhen. It is equipped with a weather station, RTK-GPS station, power management system, and other devices. Besides, the necessary equipments are installed around the lake, such as the communication station, the weather station and surveillance cameras.

I. Introduction

Autonomous sailboats, towards long range and high endurance sailing, are difficult to supply energy because they run in the open sea. They are a kind of energy-saving and eco-friendly vehicles on the ocean surface, which use wind as propulsion and only need a little energy for on-board electronics. The autonomous sailboats' superiority appears clearly among the surface vehicles in energy consumption [1]. However, up to date, the energy optimization of robotic sailboats is merely mentioned.

Existing energy optimization methods for mobile robots can be divided into three parts: (1) mechanical design [2], [3], (2) micro-electronics with low power [4]–[7], and (3) software level optimization [8]–[11]. Then two main research directions of software level are: motion planning [12]–[14] and scheduling [15]–[19].

From the perspective view of motion planning, well-known methods used in energy optimization include pseudo-spectral (PS), Extreme Seeking Control (ESC) and Linear Temporal Logic formula methodology, etc. The PS optimal control method has been applied to deal with an optimal control problem by producing an energy-optimized path between two points among static obstacles [12]. Andrea et al. use ESC strategy to realize model-free on-line motion adaption to maximize a quadcopter's flight time and distance [13]. A Linear Temporal Logic (LTL) formula methodology is presented to synthesize a motion plan for a mobile robot to ensure that the robot never gets depleted with battery charge while carrying out its mission successfully [14]. This algorithm also finds the best location for the charging station along with the optimal trajectory for the robot.

From the perspective view of scheduling, Wigstrom and Lenartson apply the state-of-the-art Mixed-Integer Nonlinear Program (MINLP) method, which models the energy consumption of the complete system to several problems to benchmark their effectiveness [15]. Benchmarks show that the Nonlinear Programming based Branch and Bound (NLP-BB) does not perform well for nonlinear scheduling problems. It is due to the weak lower bounds of the integer relaxations. For scheduling problems with nonlinear costs, Extended Cutting Plane (ECP) and in particular LP/NLP based Branch and Bound (LP/NLPBB) are shown to outperform NLP-BB. Convex modeling techniques are developed for the problem of optimal velocity control of multiple robots on given intersecting paths [16]. Riazi et al. use the peak-power energy optimization method on the manipulation planning problem [17]–[19], and they have examined their algorithms with single/two-robot cases.

A hybrid energy optimization scheme based on PS and ESC strategies is proposed to realize long-range and high-endurance sailing. We formulate energy optimization as a NLP problem of motion planning. It is to minimize the sail and rudder torques of autonomous sailboats concerning the minimum energy consumption. Specifically, the PS method

*This paper is partially supported by Project U1613226 and U1813217 supported by NSFC, China, Project 2019-INT009 from the Shenzhen Institute of Artificial Intelligence and Robotics for Society, the Shenzhen Science and Technology Innovation Commission, fundamental research grant KQJSCX20180330165912672 and PF.01.000143 from The Chinese University of Hong Kong, Shenzhen.

[1] Institute of Artificial Intelligence and Robotics for Society.
[2] The Chinese University of Hong Kong, Shenzhen.
[3] Peng Cheng Laboratory, Shenzhen.
[†] Corresponding author is Huihuan Qian, hhqian@cuhk.edu.cn

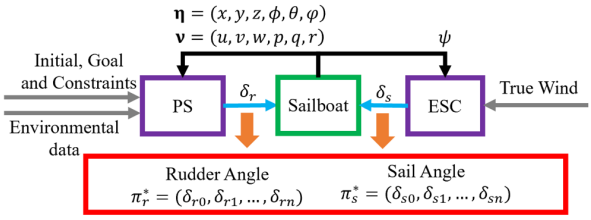

Fig. 2. Energy optimization scheme. The gray represents the input from outside. The purple boxes contain the control methods and the red box is the optimal policy generated by the optimal control method. The $\boldsymbol{\eta}$ and $\boldsymbol{\nu}$ are the vectors of velocities and positions. The ψ represents the heading angle of the robot. The π_r^* is the optimal rudder angle sequence and the π_s^* is the optimal sail angle sequence. The δ_r and δ_s are rudder angle and sail angle respectively.

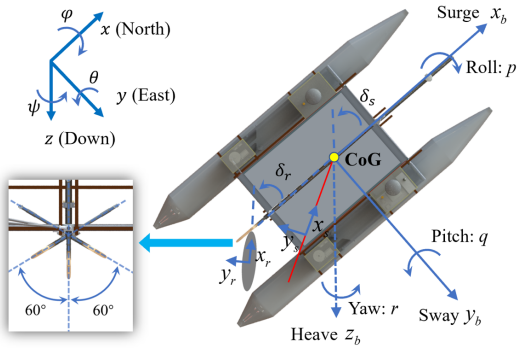

(a)

Fig. 3. Sailboat's coordinate framework, which includes the earth-fixed frame, the body-fixed frame, the sail frame and the rudder frame; the CoG represents the center of gravity. The workspace of rudder motion is in the range of $[-60°, 60°]$.

has been applied in the heading control of autonomous sailboats in surge motion, and ESC based model-free framework has been adopted in sail control.

The rest of this paper is structured as follows. Section II elaborates on the whole architecture of the energy optimization system. Section III elaborates our hybrid control algorithms. Section IV presents the simulation results. Section V shows the experimental results, analysis, and evaluation. Section VI concludes the paper.

II. Energy Management Optimization Architecture

The energy management optimization architecture is shown in Fig.2. It is a hybrid control scheme combining the PS and ESC methods. The PS is conducted on the environmental data, initial state, goal state, robot dynamics, disturbance, and constraints. A path can be determined from the initial state to the terminate state. Therefore, the rudder torque can be derived from the PS method. Then the true wind information combines heading to obtain the attack of angle, which guides ESC to find an optimal sail angle. In this paper, the goal is to generate two optimal policies π_s^* and π_r^*, in which the π_r^* is the optimal rudder angle sequence, and the π_s^* is the optimal sail angle sequence.

A. Assumption

- The environment is not with harsh wind field and water currents.
- The pitch and roll mtions of sailboat model is ignored due to the catamaran with a large base.
- The rudder and sail control is decoupled in our problem. For rudder and sail, we use the different control strategies to deal with, as mentioned in section III. They are well designed for these two specific problems.

B. Problem Formulation

We consider energy optimal sailing of autonomous sailboats between two horizontal waypoints in the obstacle-free surface area. The hybrid controller is designed to drive the sailboat from the initial position $\mathbf{x}_0$ to the final position $\mathbf{x}_f$. The energy consumed by the motors is defined as:

$$J(\mathbf{x}_f - \mathbf{x}_0, \{T_k^i\}) = \sum_{k=0}^{n-1} (\sum_{i=1}^{2} P(T_k^i) \cdot \frac{t}{n}) \tag{1}$$

where T_k^i represents the input signal sequence, such as the motor signal. P is the electronic property corresponding to the power of actuator. In our experiment, the P is a power function of the certain device. The i is the index for timestamp; the k is used to identify the device unit such as motor, sensors; the n is the samples during the whole period, and t is the travel time.

The minimization of J in Equation (1) is subject to:

- 4 DOF system dynamic is described in Equation (6)
- The inequalities give the state and input constraints: $C_{\min} \leq C_k \leq C_{\max}$, where $C_k = [T_k^i, y_k, z_k, \phi_k, \theta_k, \psi_k]^T$, $(\cdot)_{min}$ and $(\cdot)_{max}$ are the minimum and maximum of the corresponding variables.
- The time boundary on the initial and final state.

In this paper, the sailboat's energy consumption of the rudder and sail are reformulated with respectively in Equation (2) J_R and (3) J_S. As the system dynamics are highly nonlinear in our model, the motion of sailboat is hard to deal with. Thus, we take J_R into consideration and reformulate it as a NLP problem. Therefore, the rudder can be controlled and the motion of sailboat is simplified.

$$J_R(\mathbf{x}_f - \mathbf{x}_0, T_r) = \sum_{k=0}^{n-1} (P(T_r) \cdot \frac{t}{n}) \tag{2}$$

where J_R represents the energy cost on the rudder motor.

$$J_S(\mathbf{x}_f - \mathbf{x}_0, T_s) = \sum_{k=0}^{n-1} (P(T_s) \cdot aoa(\frac{t}{n})) \tag{3}$$

where J_S depicts the energy cost on the sail motor. The $aoa(\cdot)$ is the accumulated time with the attack of angle changing.

Besides, the energy in other components, J_O, can be formulated in Equation (4),

$$\begin{aligned} J_O(\mathbf{x}_f - \mathbf{x}_0, T_r, T_s, T_o) &= (n_{motor} + 1) * P(T_o) \cdot \frac{t}{n} \\ &= \sum_{k=0}^{n-1} (\|P(T_{s,r}) - P_\mu(T_{s,r})\|_2 / P_{max} + 1) \cdot P(T_o) \cdot \frac{t}{n} \end{aligned} \tag{4}$$

TABLE I

PARAMETERS OF MATHEMATICAL MODEL

x, y, z	Position on the n-frame
x_s, y_s, z_s	Position on the s-frame
x_r, y_r, z_r	Position on the r-frame
L, D	Lift and drag force on the foil
m	Total mass of the sailboat
α	Angle of attack on b-frame
α_{aw}	Apparent wind angle on b-frame
α_{tw}	True wind angle on b-frame
α_{ar}	Apparent rudder angle on b-frame
δ	Sail and rudder angle on b-frame
x_m	The x-coordinate of the mast on b-frame
x_{sm}	Distance between the mast and the sail's CoE

where the n_{motor} is the noise variable acting on the motors. It affects the other components as a shake. T_o is the configuration signal sequence of sensors. In most cases, the signals are constant. The $P(T_{s,r})$ is the total power on the sail motor and rudder motor. The $P_\mu(T_{s,r})$ is the mean of the $P(T_{s,r})$. Besides, P_{max} represents the maximum power of the motors.

Then, the sailboat's energy consumption is in Equation (5),

$$J_K(\mathbf{x}_f - \mathbf{x}_0, \{T_k^i\}) = J_R + J_S + J_O \tag{5}$$

where J_K is the total energy cost combines J_R, J_S and J_O in Equation. (2-4). $P(T_R)$ and $P(T_S)$ will be conducted by the hybrid control scheme in Section III. Therefore, the energy optimization problem has been converted to generate minimize torques of the sailboats.

C. Mathematical Model of Catamaran Sailboats

We establish a simplified 4-DOF model of kinematics and dynamics of catamaran sailboat based on [1], [20], [21]. Here, the heave and pitch motions are neglected. The earth-fixed (n-frame) and body-fixed (b-frame) coordinate frames are introduced in Fig.3(a). The parameters of different components are defined in Table I.

Based on the coordinate frames and parameter notations, the movement of an autonomous sailboat can be derived, which is according to the Newton-Euler equations of motion for a rigid body in Equation (6) [21],

$$\begin{cases} \boldsymbol{M}\dot{\boldsymbol{\nu}} + \boldsymbol{C}(\boldsymbol{\nu})\boldsymbol{\nu} + \boldsymbol{D}(\boldsymbol{\nu})\boldsymbol{\nu} + g(\boldsymbol{\eta}) = \boldsymbol{\tau} \\ \dot{\boldsymbol{\eta}} = J(\boldsymbol{\eta})\boldsymbol{\nu} \end{cases} \tag{6}$$

where $\boldsymbol{M}$ is the total mass, $\boldsymbol{C}(\boldsymbol{\nu})$ is the system Coriolis-centripetal matrix, $\boldsymbol{D}(\boldsymbol{\nu})$ is the system damping matrix, $g(\boldsymbol{\eta})$ is the hydrostatic force. $J(\boldsymbol{\eta})$ is the coordinate transformation between the b-frame and n-frame. In this paper, the calculation of $\boldsymbol{C}(\boldsymbol{\nu})$, $\boldsymbol{D}(\boldsymbol{\nu})$, $g(\boldsymbol{\eta})$, and $J(\boldsymbol{\eta})$ are not shown in details.

Lift and drag forces on foils are:

$$L = \frac{1}{2}\rho A v_a^2 C_L(\alpha) \tag{7}$$

$$D = \frac{1}{2}\rho A v_a^2 C_D(\alpha) \tag{8}$$

where ρ is the density of the fluid surrounding the foil, A denotes the surface of the foil, v_a means the apparent velocity of the fluid, $C_L(\alpha)$ and $C_D(\alpha)$ are the dimensionless lift and drag coefficients as a function of the angle of attack α, respectively.

$\boldsymbol{\tau}$ is the vector with the resulting propulsive forces of the sailboat, and it contains the force of sail and rudder,

$$\boldsymbol{\tau} = \boldsymbol{\tau}_s + \boldsymbol{\tau}_r \tag{9}$$

where $\boldsymbol{\tau}_s$ is the sail resulting force, and $\boldsymbol{\tau}_r$ is the rudder resulting force.

$$\boldsymbol{\tau}_s = \begin{bmatrix} L_s \sin\alpha_{aw} - D_s \cos\alpha_{aw} \\ L_s \sin\alpha_{aw} + D_s \cos\alpha_{aw} \\ L_s \sin\alpha_{aw} + D_s \cos\alpha_{aw}|z_s| \\ -(L_s \sin\alpha_{aw} - D_s \cos\alpha_{aw})x_{sm}\sin\delta_s \\ L_s \sin\alpha_{aw} + D_s \cos\alpha_{aw}(x_m - x_{sm}\cos\delta_s) \end{bmatrix} \tag{10}$$

where L_s and D_s are corresponding to the lift and drag force on the sail. δ_s is the sail angle on the b-frame,

$$\boldsymbol{\tau}_r = \begin{bmatrix} L_r \sin\alpha_{ar} - D_r \cos\alpha_{ar} \\ L_r \sin\alpha_{ar} + D_r \cos\alpha_{ar} \\ L_r \sin\alpha_{ar} + D_r \cos\alpha_{ar}|z_r| \\ -(L_r \sin\alpha_{ar} - D_r \cos\alpha_{ar})|x_r| \end{bmatrix} \tag{11}$$

where L_r and D_r corresponding to the lift and drag force on the rudder.

III. HYBRID CONTROL SCHEME

This hybrid control scheme is a combination of PS and ESC method. PS method is used in heading control, which includes the path planning and the torque generation. Another control pipeline is the ESC, which is mainly used to deal with the sail. The optimal extremum sail angle exists and can be found out with the ESC method.

A. PS in Heading Control

For an optimal control problem, the state, control, and system dynamics are the key elements. The cost function is defined as the minimum force or torque to make sure the minimum energy consumption. The solution framework is shown in Fig.4.

Notably, the objective function is included boundary and integral function, which is minimized subjected to the established dynamic model, time boundary on initial state t_0 and final state t_F, state boundary $\mathbf{x}(t_0)$, $\mathbf{x}(t_F)$, etc.

In our work, the global environment is fitted by the weather stations installed around the test place. The wind field can be described as in Equation (12).

$$h(x, y) = 2 * y + \sin(3 * x) \tag{12}$$

where the x and y are in the earth-fixed coordinate frame. The dark color shows a high wind speed area [6(b), 6(d)].

The slope in the direction of travel based on the dynamic model can be derived in Equation (13).

$$\nabla = dx * \frac{\partial h}{\partial x} + dy * \frac{\partial h}{\partial y} \tag{13}$$

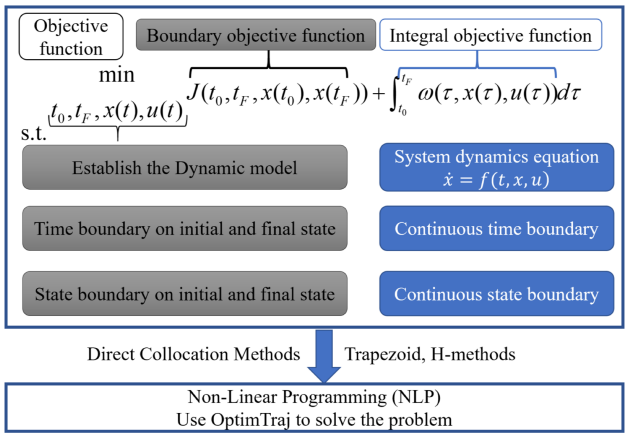

Fig. 4. Non-linear programming framework with the optimization problem. It uses the solution configuration in this problem with direct collocation methods, trapezoid and H-methods to calculate the optimal policy.

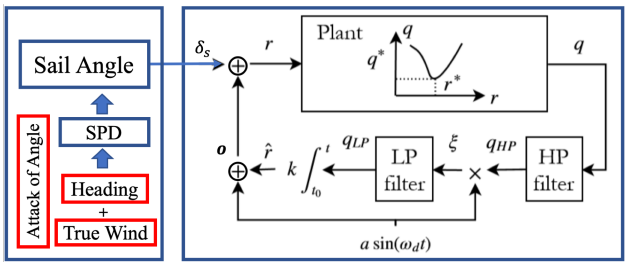

Fig. 5. The block diagram of the feedback scheme based on Extreme Seeking control. The reference input is a sail angle, which is obtained from the attack of angle (the heading angle concerning the true wind). Especially, the heading angle is generated from Fig.4. Then the ESC can be used to calculate the output based on the feedback information and the perturbation, which guides the sail angle.

where the dx and dy is the differential of the x and y w.r.t time, which can be obtained by the dynamic model. The $\frac{\partial h}{\partial x}$ and $\frac{\partial h}{\partial y}$ are the partial differential w.r.t x and y.

The objective function is trading off the motor torque minimization, and wind speed area maximization. Hereby, two objective functions have been considered. The first one ${}^1J$ is with maximum high wind speed, and slope information, as shown in Equation (14). It is based on the gradient desent (GD) method [22]. The other one is our objective function ${}^2J$ with torque optimization.

$$ {}^1J = \log^{-1}(\|h(x,y)\|_2) + \lambda_1 \|\nabla\|_2^{-1} \tag{14} $$

${}^2J$ is optimized with the $\|u\|_2^2$

$$ {}^2J = \log^{-1}(\|h(x,y)\|_2) + \lambda_1 \|\nabla\|_2^{-1} + \lambda_2 \|u\|_2^2 \tag{15} $$

The based line is the ${}^1J$ in the gradient descent method. Our objective function ${}^2J$ is a fine-tuned cost with minimized input torques $\|u\|_2^2$.

Thus, the direct collocation (DC) method [23] is used to get the global optimal solution. We consider the maneuvering from $(x_0, y_0) = (0, 0)$ to $(x_f, y_f) = (10, 8)$ as the unit m, the control variable $u_0 = 0$. The state equation is discretized into 150 segments and approximated with the trapezoid rule to guarantee the optimality and robustness. The constraints are set as $C_{max} = -C_{min} = [1.5, 20, 5, 0.2 * pi, 2 * pi, 0.1 * pi]^T$. Besides, $\lambda_1 = 0.05$, and $\lambda_2 = 0.001$.

B. ESC Control Method in Sail Control

Sailing control is based on tuning the sail angle to fit the current state. For different sailboats, there is no general model to calculate the accurate sail model. However, there exists some traditional methods to derive an abstract model [24] based on the ESC.

The ESC is a continuous-time version of perturbation and observation. Instead of just taking fixed discrete steps, it can take bigger or smaller steps depending on the slope or the gradient of the objective function. It is a kind of generalization with faster tracking because it takes more significant steps when having a higher slope. There are also provable guarantees on the case when this will and will not converge for dynamical systems. It is useful to illustrate what is happening here for a static objective function with an instantaneous dynamic.

ESC allows us to find an unknown, time-varying plant operating point $r^*(t)$, which maximizes or minimizes a given plant output $q(t)$. The optimal setpoint is found by applying a small periodic perturbation $asin(\omega_d t)$ to the current reference $\hat{r}(t)$ by monitoring the changes of the plants output at the given disturbance frequency ω_d.

The diagram of ESC is shown in Fig.5. The input reference value is a sail angle which is obtained based on the speed polar diagram (SPD) from the attack of angle [25]. The given plant is built based on the abstract model in [24]. Then the controller can generate the new value r as the sail torque by combining the perturb dynamics. The perturb dynamic can be designed as a sine or cosine function. According to our objective function, we designed a sine function with 20 rad/s period and the 0.15 amplitude.

IV. Simulation Results

In the simulation, we mainly test our energy optimization scheme in a downwind scenario and windward scenario with GD method and our method, as shown in Fig.6.

Downwind Scenario s_1: In this scenario, the sailboat sails along with the wind. The sailboat sails from the start point p_{10} to the goal point g_1. In Fig.6(b), the sailboat arrives at the g_1 by adapting the sail and rudder timely. From Fig. 6(a), we can verify the success with the truth that both surge and sway coordinates have increased. The torque is changing to catch the wind and then slightly go back to achieving the goal.

Windward Scenario s_2: The wind blows from the bottom direction. The sailboat sails from the start point p_{20} to the goal point g_2. In Fig.6(d), the sailboat also gets to the goal position. The goal is in the right-down direction, so the surge coordinate increase, and the sway coordinates decrease. The torque is changing slightly to tacking against the wind and then turn back to achieve the goal.

Sail Adaption Tuning: The sail is adjusted based on the attack of angle and ESC method. The goal is to harness

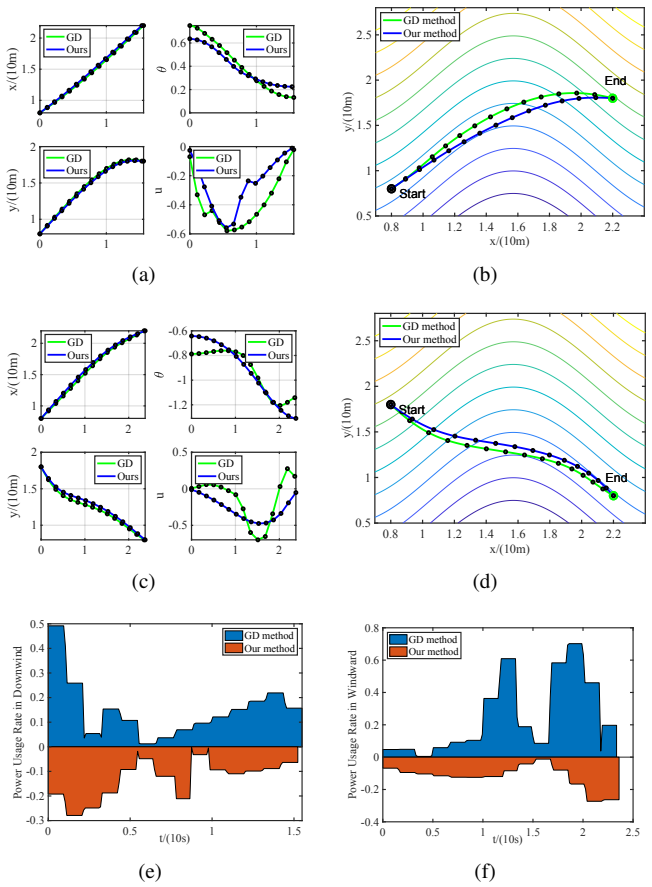

Fig. 6. Simulation results in different environments. (a) results of the downwind scenario, x position, the heading angle, y position, and the torque input with respect to timestamps. (b) is the simulation trajectory of oceanVoy in downwind. (c) results of the windward scenario, x position, the heading angle, y position, and the torque input with respect to timestamps. (d) is the simulation trajectory of oceanVoy in windward. The darker light shows the higher wind speed than a light line. Besides, the green line represents the GD method, and the blue line illustrates our method. (e) and (f) depict the power usage rate. The power usage rate is the ratio between current power and maximum power. The blue area in positive axis is based on GD method, and the red area in negative axis is ours. The positive and negative area is used to distinguish two methods.

enough wind for propulsion. The results show that the autonomous sailboat can work in this given environment. The control value can be iterated computing to obtain the minimum control input. Therefore, it can be transferred to real-world sailboat.

Energy Analysis: From Fig.6(e) and 6(f), our method is smaller than the GD method in power usage. It means that our approach decreased the power while finishing the same goal. Moreover, from the statistic result, the variance and accumulated power efficiency are smaller in our method than the GD method. Therefore, we valid our performance and advantage in the energy planning.

V. Real-World Implementation and Evaluation

A. Hardware Design and OceanVoy Configuration

OceanVoy: The OceanVoy is a catamaran sailboat, which is retrofitted from a minicat310 sailboat with a size of

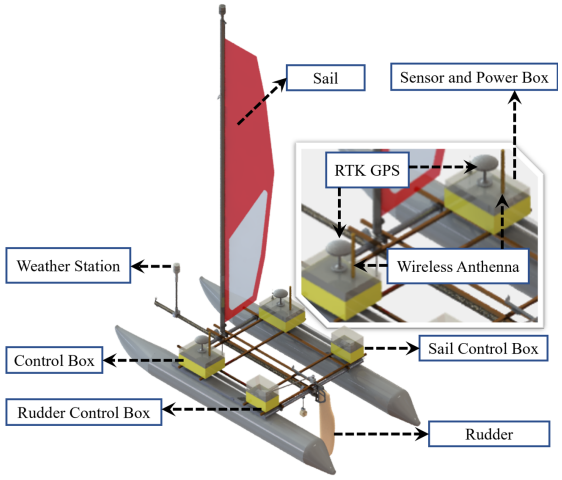

Fig. 7. The configurations of OceanVoy.

310cm*140cm*380cm. It is equipped with a rudder, a sail, a control box, a power box, an RTK GPS, a wireless antenna, and a weather station, etc., as shown in Fig.7. Besides, the power management system is placed in the power box.

Rudder & Sail Systems: The rudder is retrofitted with a link and worm gearbox. An encoder is equipped to obtain the feedback of absolute rudder angle δ_r. The mechanism design can be shown in Fig.3. The workspace of the rudder δ_r is within $[-60°, 60°]$.

The sail is controlled with a worm gearbox. The winch is used to tighten and release the rope. The relevant position with the rudder control box and sail control box is delicately designed to keep balance.

B. Shenxian Lake Environment and Configuration

The experiments are conducted in Shenxian Lake, CUHKSZ, using OceanVoy, as shown in Fig.8. According to historical data of offshore weather stations, we modeled the wind condition as different level-sets. Then we choose the proper time to implement the experiment when the wind filed is similar to the simulation. The average wind speed is 3 knots to 4 knots.

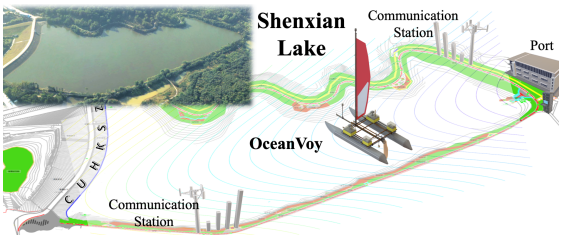

Fig. 8. The environment and surrounding equipment in Shenxian Lake.

C. Experimental Reliability Validation

From the repeated tests, we pick up two representative scenarios to illustrate the reliability of motion planning. It includes the tracking error, sailing distance, and sailing time. With this prerequisite result, we can evaluate the energy efficiency in the the next subsection (V-D).

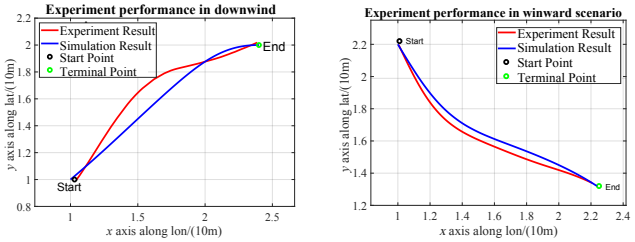

(a) (b)

Fig. 9. The experiment validation v.s. the simulation result. In the experiment, oceanVoy can track the trajectory with the mean error less than 1.5m.

In Fig.9, oceanVoy sails from start point to terminal. The red line represents the experiments, which is the true path of oceanVoy. The blue line corresponds to cases in simulation, as shown in Fig.6. They are all able to reach the goal and follow the most of paths. For specification in traveling, in Fig.9(a), the total distance is 17.494m in the simulation v.s. 29.455m in the experiment. It consumes 8s in the simulation and 10s in the experiment. In Fig.9(b), the total distance is 18.047m in the simulation v.s. 20.625m in the experiment. It consumes 4s in the simulation and 4.5s in the experiment. In Fig.9(a) and 9(b), the mean error is $2m$ and $1m$ respectively.

D. Energy Efficiency Evaluation

We evaluated the effectiveness of our optimization method based on the simulation and experiment results. In the simulation, the total energy is calculated by Equation (5). In the experiments, the total energy is collected via the battery management system on the OceanVoy with the timestamps. Therefore, the energy consumption for quantitative results is as shown in Table II, which are based on the statistics of simulation and experiments.

TABLE II

QUANTITATIVE DATA IN SIMULATION AND EXPERIMENT RESULTS

Scenarios	*downwind*			*windward*		
†Functions	${}^1J_k$	${}^2J_k$	%	${}^1J_k$	${}^2J_k$	%
Simulation	$114.6J$	$110.7J$	3.4	$69.9J$	$62.4J$	10.8
Experiment	$145.9J$	$141.6J$	3.0	$80.9J$	$72.4J$	10.5

†Functions: J_k is the total consumed energy in Equation (5). Notably, the footnotes ^{1} and ^{2} represent method based on Equation (14-15).

From Table II, we can obtain that the ${}^2J_k$ is better than ${}^1J_k$ in the downwind situation. Around 3% of energy is saved. In the windward situation, the ${}^2J_k$ is also better than ${}^1J_k$. It can save around 10% energy. The total improvement for our method is approximate 7%, from the Table. II.

It can be seen that the windward is more energy-saving than downwind since the sailboat is more stable in the windward environment with a steady lift and drag. For the downwind situation, there is turbulent to affect the sailboat. Moreover, it is more sensitive to the wind when the sailboat is downwind. Thus, energy is more consumed.

The energy is slightly higher in experiment than simulation. It may come from the disturbance from the un-predicted environment, especially the water current. Another reason maybe the power of the electronic system exists the joggling, which produces the error in estimated power.

Therefore, it can be concluded that our hybrid schema of the optimization algorithm is valid for robotic sailing based on the validation and evaluation with quantitative energy consumption. It is a fundamental and significant step for us to explore the ocean in long-range and long duration in the future.

VI. Conclusions

In this paper, we have proposed a hybrid energy planning method. In this scheme, pseudo-spectral (PS) optimal control method is used in heading control, and a model-free framework guided by extreme seeking control (ESC) is used in sail control. We implemented the simulation results into the real-world. As a result, the energy can be saved 7% as the mean value than the GD method. Besides, it is validated that the path can be tracked in $1.5m$ error. Finally, we proved that our energy optimization algorithm is effective on oceanVoy.

In the future, we are continuing to study the energy planning in long-range and long-duration sailing, and in the extreme weather condition. This kind of energy-efficient autonomous sailing robots will be released to sail in the ocean for exploration and exploitation.

References

[1] D. H. dos Santos and L. M. G. Goncalves, "A gain-scheduling control strategy and short-term path optimization with genetic algorithm for autonomous navigation of a sailboat robot," *International Journal of Advanced Robotic Systems*, vol. 16, no. 1, p. 1729881418821830, 2019.

[2] R. D'Sa, D. Jenson, T. Henderson, J. Kilian, B. Schulz, M. Calvert, T. Heller, and N. Papanikolopoulos, "Suav: Q-an improved design for a transformable solar-powered uav," in *2016 IEEE/RSJ International Conference on Intelligent Robots and Systems (IROS)*. IEEE, 2016, pp. 1609–1615.

[3] W. Kraus, A. Spiller, and A. Pott, "Energy efficiency of cable-driven parallel robots," in *2016 IEEE International Conference on Robotics and Automation (ICRA)*. IEEE, pp. 894–901.

[4] S. W. Keckler, W. J. Dally, B. Khailany, M. Garland, and D. Glasco, "GPUs and the future of parallel computing," *IEEE Micro*, vol. 31, no. 5, pp. 7–17, sep 2011.

[5] S. Mittal, S. Gupta, and S. Dasgupta, "Fpga: An efficient and promising platform for real-time image processing applications," in *National Conference On Research and Development In Hardware Systems (CSI-RDHS)*, 2008.

[6] H. Lee and Y. Choi, "A new actuator system using dual-motors and a planetary gear," *IEEE/ASME Transactions on Mechatronics*, vol. 17, no. 1, pp. 192–197, feb 2012.

[7] J. Kim, H. Yeom, F. C. Park, Y. I. Park, and M. Kim, "On the energy efficiency of cvt-based mobile robots," in *Proceedings 2000 ICRA. Millennium Conference. IEEE International Conference on Robotics and Automation. Symposia Proceedings (Cat. No. 00CH37065)*, vol. 2. IEEE, 2000, pp. 1539–1544.

[8] P. Ondruska, C. Gurau, L. Marchegiani, Chi Hay Tong, and I. Posner, "Scheduled perception for energy-efficient path following," in *2015 IEEE International Conference on Robotics and Automation (ICRA)*. IEEE, pp. 4799–4806.

[9] J. Yu, F. Zhang, A. Zhang, W. Jin, and Y. Tian, "Motion parameter optimization and sensor scheduling for the sea-wing underwater glider," *IEEE journal of oceanic engineering*, vol. 38, no. 2, pp. 243–254, 2013.

[10] M. Wei and V. Isler, "Coverage path planning under the energy constraint," in *2018 IEEE International Conference on Robotics and Automation (ICRA)*. IEEE, pp. 368–373.

[11] M. De Stefano, R. Balachandran, A. M. Giordano, C. Ott, and C. Secchi, "An energy-based approach for the multi-rate control of a manipulator on an actuated base," in *2018 IEEE International Conference on Robotics and Automation (ICRA)*. IEEE, 2018, pp. 1072–1077.

[12] G. Bitar, M. Breivik, and A. M. Lekkas, "Energy-optimized path planning for autonomous ferries," *IFAC-PapersOnLine*, vol. 51, no. 29, pp. 389–394, 2018.

[13] A. Tagliabue, X. Wu, and M. W. Mueller, "Model-free online motion adaptation for optimal range and endurance of multicopters," p. 7.

[14] T. Kundu and I. Saha, "Energy-aware temporal logic motion planning for mobile robots," in *2019 International Conference on Robotics and Automation (ICRA)*. IEEE, 2019, pp. 8599–8605.

[15] O. Wigstrom and B. Lennartson, "Sustainable production automation - energy optimization of robot cells," in *2013 IEEE International Conference on Robotics and Automation*. IEEE, pp. 252–257.

[16] O. Wigstrom, N. Murgovski, S. Riazi, and B. Lennartson, "Computationally efficient energy optimization of multiple robots," in *2017 13th IEEE Conference on Automation Science and Engineering (CASE)*. IEEE, pp. 515–522.

[17] S. Riazi, O. Wigstrom, K. Bengtsson, and B. Lennartson, "Energy and peak power optimization of time-bounded robot trajectories," vol. 14, no. 2, pp. 646–657.

[18] S. Riazi, K. Bengtsson, R. Bischoff, A. Aurnhammer, O. Wigstrom, and B. Lennartson, "Energy and peak-power optimization of existing time-optimal robot trajectories," in *2016 IEEE International Conference on Automation Science and Engineering (CASE)*. IEEE, pp. 321–327.

[19] S. Riazi, K. Bengtsson, O. Wigstrom, E. Vidarsson, and B. Lennartson, "Energy optimization of multi-robot systems," in *2015 IEEE International Conference on Automation Science and Engineering (CASE)*. IEEE, pp. 1345–1350.

[20] D. Krammer, "Modeling and control of autonomous sailing boats," Ph.D. dissertation, Masters thesis, ETH Zürich, Switzerland, 2014.

[21] T. I. Fossen, *Guidance and control of ocean vehicles*. John Wiley & Sons Inc, 1994.

[22] S. Ruder, "An overview of gradient descent optimization algorithms," *arXiv preprint arXiv:1609.04747*, 2016.

[23] O. Von Stryk and R. Bulirsch, "Direct and indirect methods for trajectory optimization," *Annals of operations research*, vol. 37, no. 1, pp. 357–373, 1992.

[24] H. Saoud, M.-D. Hua, F. Plumet, and F. B. Amar, "Optimal sail angle computation for an autonomous sailboat robot," in *2015 54th IEEE Conference on Decision and Control (CDC)*. IEEE, 2015, pp. 807–813.

[25] F. Plumet, C. Petres, M.-A. Romero-Ramirez, B. Gas, and S.-H. Ieng, "Toward an autonomous sailing boat," *IEEE Journal of Oceanic Engineering*, vol. 40, pp. 397–407, 04 2015.